

Supplementary material:

Crystal structures of the effector-binding domain of repressor CggR from *Bacillus subtilis* reveal ligand-induced structural changes upon binding of several glycolytic intermediates.

Pavčina Řezáčová^{1,3,4*}, Milan Kožíšek³, Shiu F. Moy², Irena Siegllová^{3,4}, Andrzej Joachimiak², Mischa Machius¹, Zbyszek Otwinowski¹

Table S1: Protein-ligand binding parameters

Crystal	Free	FBP co-crystal		GAP/DHAP co-crystal		G6P co-crystal		F6P co-crystal	
		DHAP	FBP	DHAP	DHAP	G6P	G6P	F6P	F6P
Ligand buried ASA ^a (Å ²)	292.0	293.7	426.0	295.6	296.1	376.1	373.7	358.1	358.5
Ligand buried ASA ^a (%)	92.8	93.1	90.1	93.8	94.3	96.9	95.8	92.5	92.6
Interface protein polar atoms ^b (%)	43.3	43.1	49.0	44.8	46.4	41.9	43.4	42.3	45.2
Bridging water molecules ^b	6	6	9	6	5	4	4	4	4
Gap Volume Index ^c	0.84	0.84	1.11	0.79	0.75	0.49	0.64	0.53	0.64

^a accessible surface area (ASA) was determined by PISA server (Krissinel & Henrick, 2005).

^b determined by Protein-protein interaction server (Jones & Thornton, 1996).

^c Gap volume index is defined as Gap volume / interface ASA, where gap volume is the volume of the gaps between the two interacting subunits. This parameter gives a measure of the complementarity of the interacting surfaces.

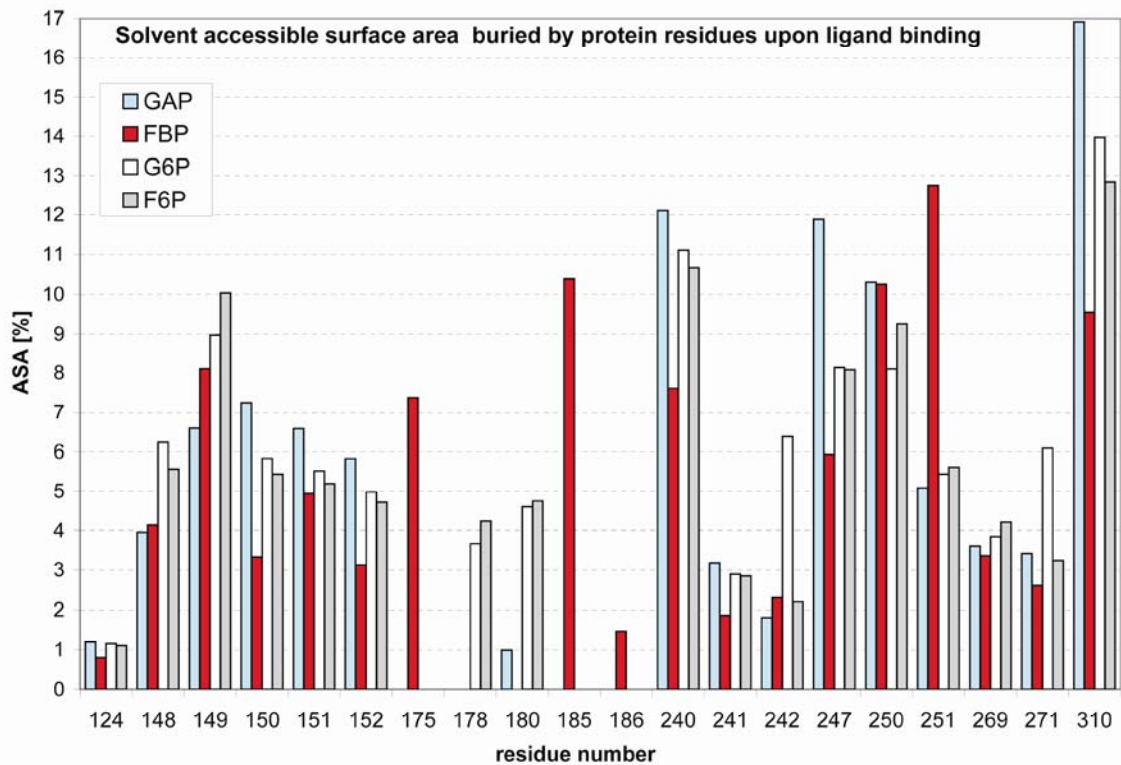


Figure S1: Solvent accessible surface area (ASA) buried by protein residues upon ligand binding. Determined by using Protein-protein interaction server (Jones and Thornton, 1996)

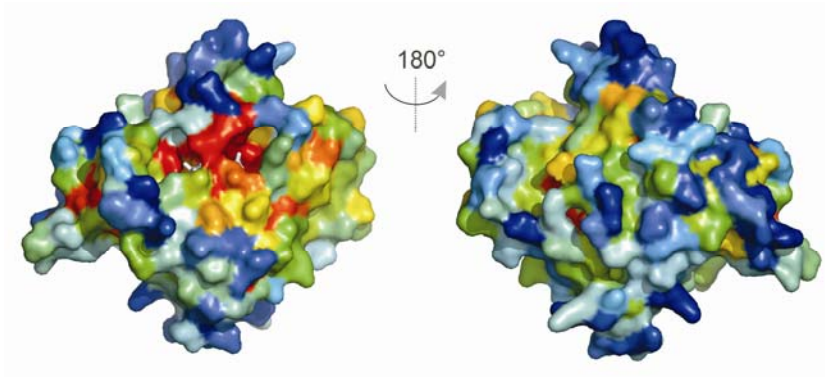


Figure S2: Conservation of C-CggR surface residues.

The solvent-accessible surface of the CggR effector domain colored by residue conservation in 59 closely homologous sequences. The surface is colored in rainbow colors, with blue representing a sequence identity of 10% or lower and red representing a sequence identity of over 90%. Bound FBP is shown as white sticks.

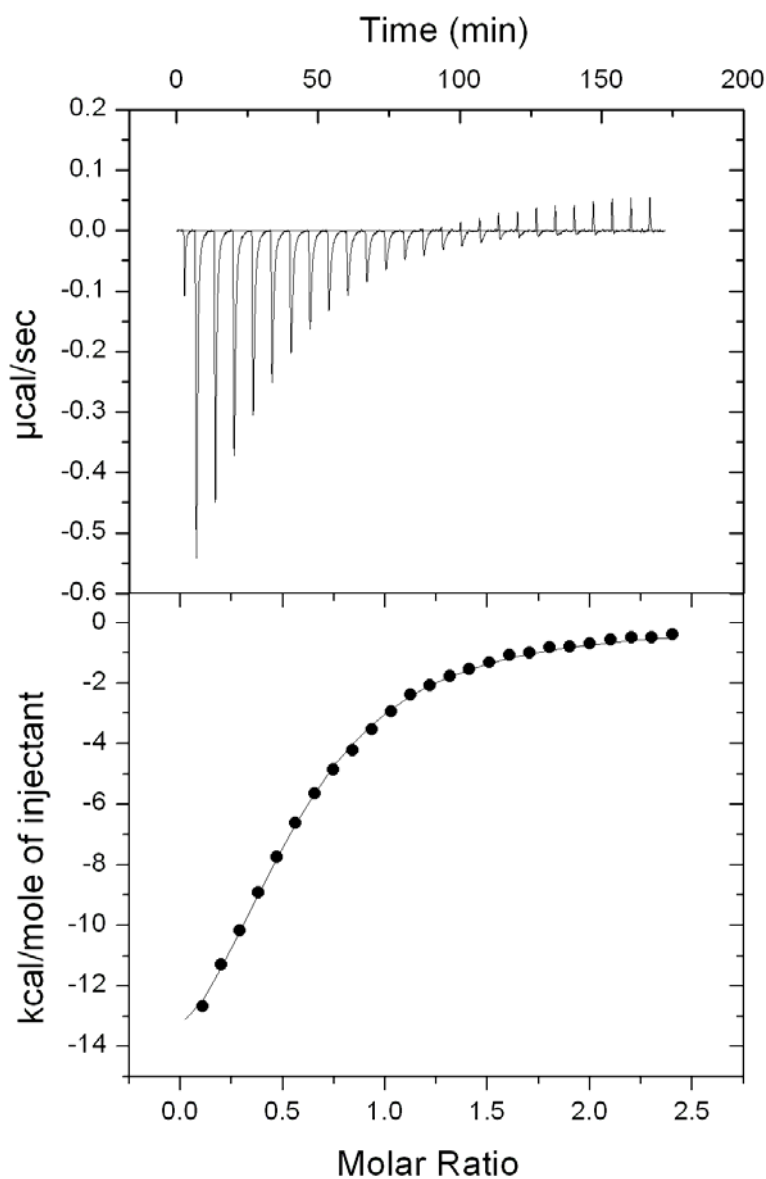


Figure S3: Isothermal titration calorimetry (ITC) profile of FBP binding to C-CggR preloaded with DHAP (the preparation used for crystallographic studies).

The C-CggR concentration in the cell was 18.83 μM and the FBP concentration in the injection was 350 μM . The fit corresponds to a single-site binding model with $K_d = 4.26 \mu\text{M}$ and stoichiometry 0.55.

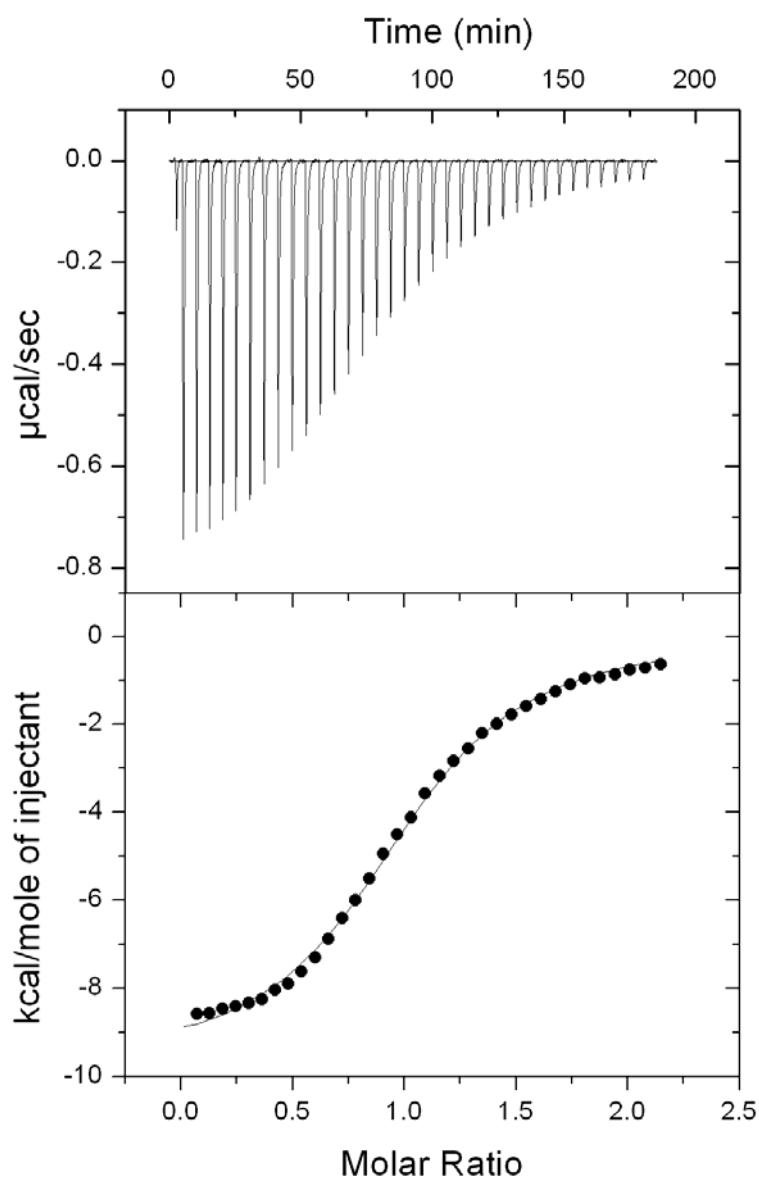


Figure S4: ITC profile of FBP binding to C-CggR ligand-free apo-protein.

The C-CggR concentration in the cell was 27.65 μM and the FBP concentration in the injection was 375 μM . The fit corresponds to a single-site binding model with average $K_d = 2.87 \mu\text{M}$ and stoichiometry 1.05.

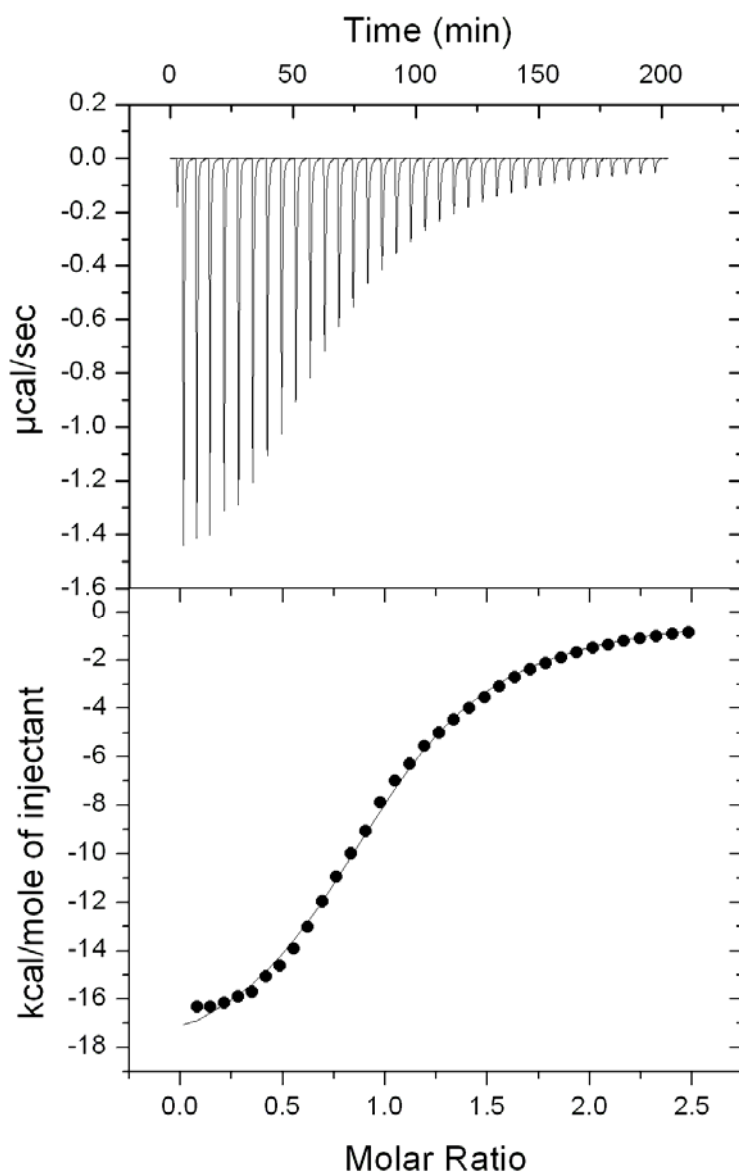


Figure S5: ITC profile of DHAP binding to C-CggR ligand-free apo-protein.

The C-CggR concentration in the cell was 32.63 μM and the DHAP concentration in the injection was 360 μM . The fit corresponds to a single-site binding model with $K_d = 3.34 \mu\text{M}$ and stoichiometry 1.03.

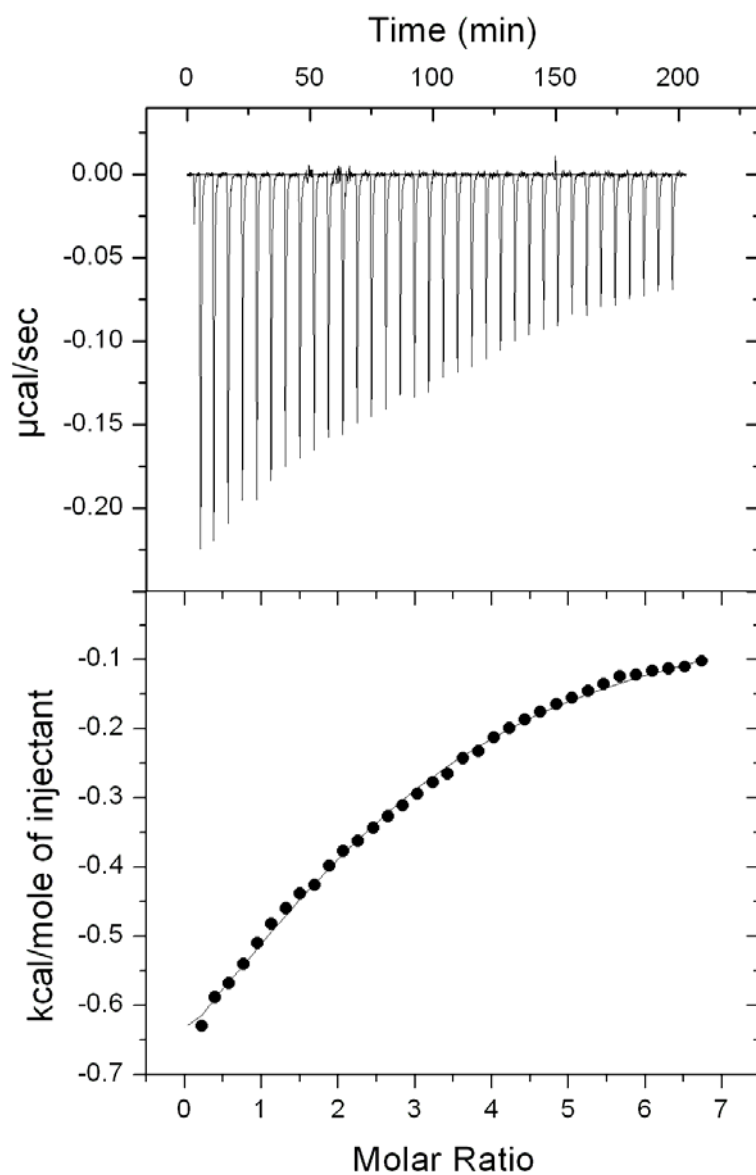


Figure S6: ITC profile of GAP binding to C-CggR ligand-free apo-protein.

The C-CggR concentration in the cell was 33.4 μM and the GAP concentration in the injection was 1 mM. The fit corresponds to a single-site binding model with $K_d = 63.3 \mu\text{M}$ and stoichiometry 2.86.

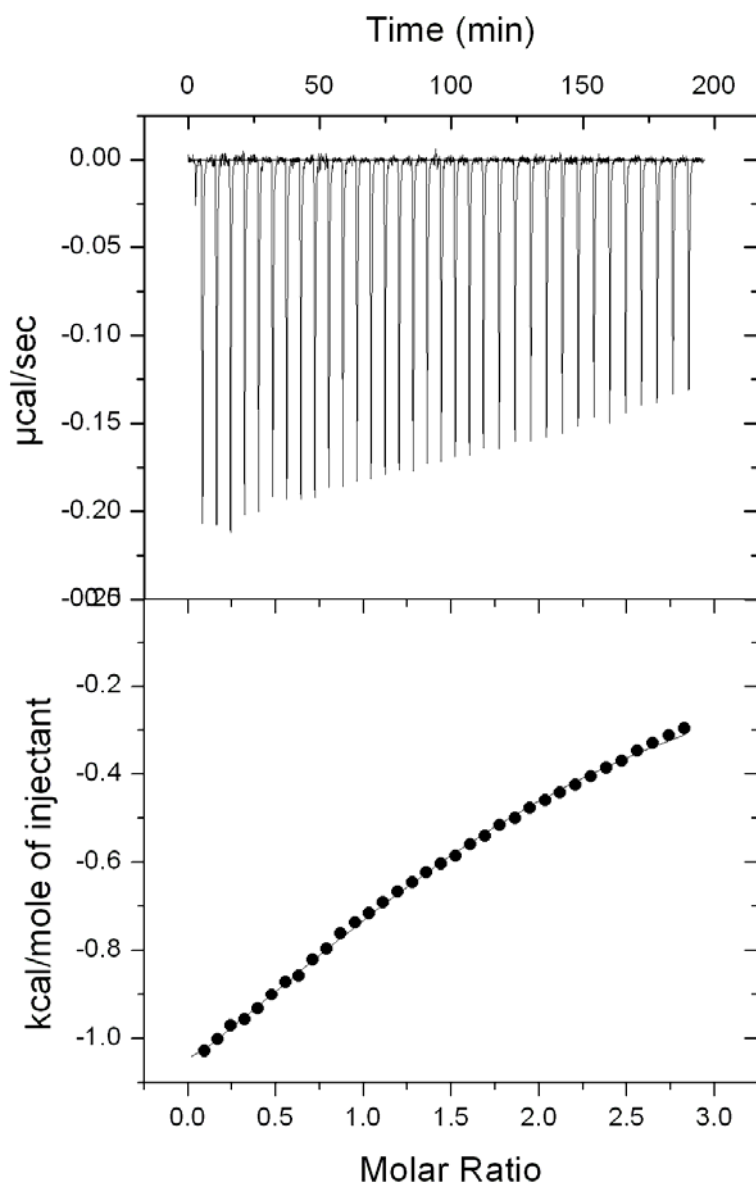


Figure S7: ITC profile of G3P binding to C-CggR ligand-free apo-protein.

The C-CggR concentration in the cell was $31.2 \mu\text{M}$ and the G3P concentration in the injection was $400 \mu\text{M}$. The fit corresponds to a single-site binding model with $K_d = 27.59 \mu\text{M}$ and stoichiometry 1.97.

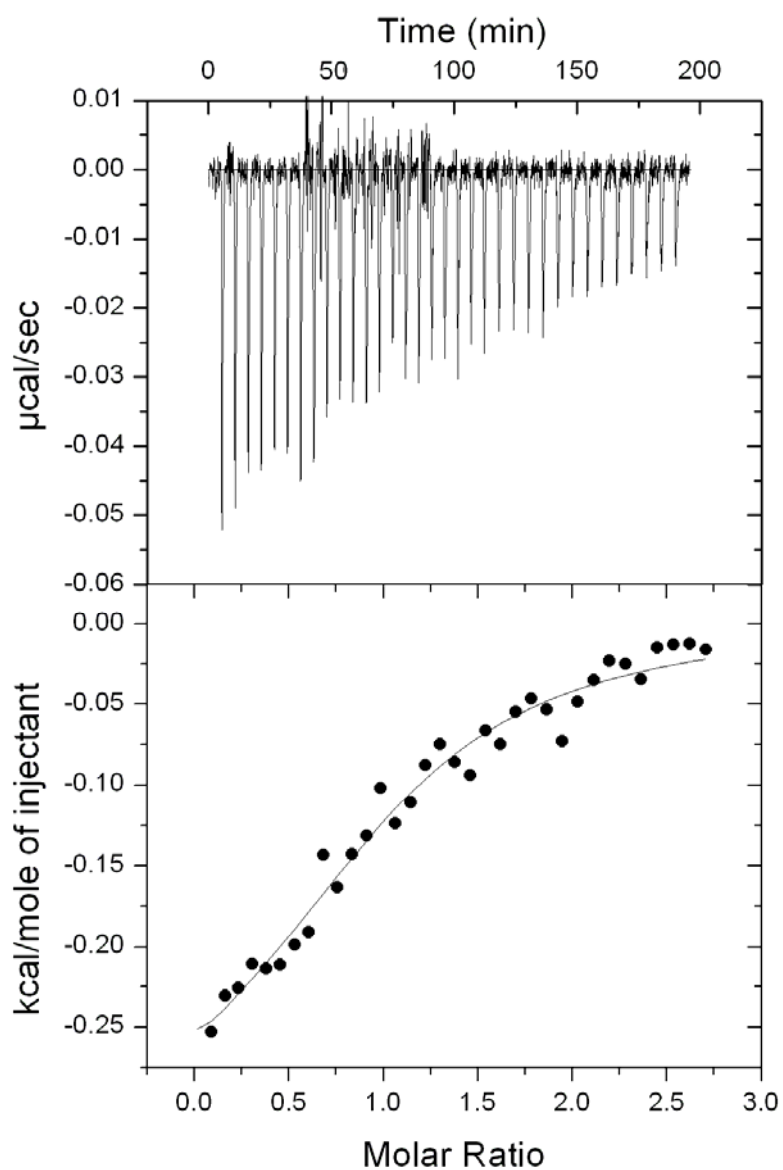


Figure S8: ITC profile of G6P binding to C-CggR ligand-free apo-protein.

The C-CggR concentration in the cell was 32.4 μM and the G6P concentration in the injection was 390 μM . The fit corresponds to a single-site binding model with $K_d = 10.98 \mu\text{M}$ and stoichiometry 0.98.

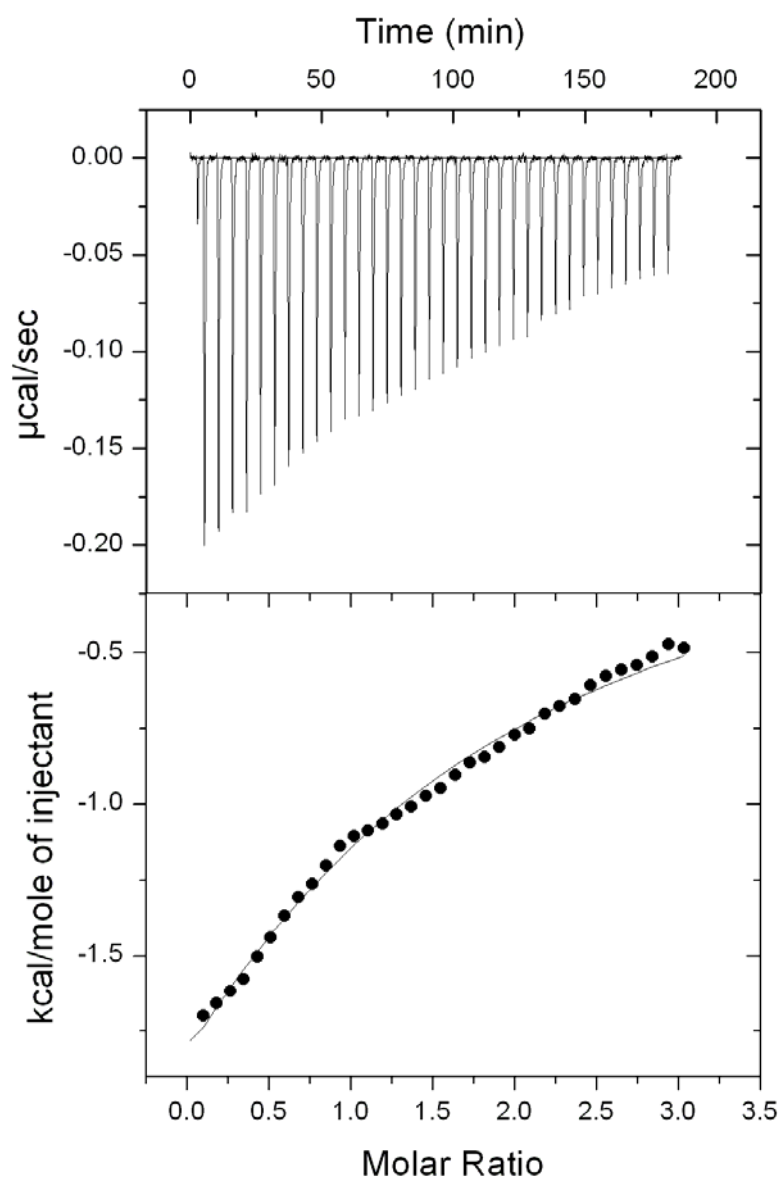


Figure S9: ITC profile of F6P binding to C-CggR ligand-free apo-protein

The C-CggR concentration in the cell was $31.5 \mu\text{M}$ and the F6P concentration in the injection was $425 \mu\text{M}$. The fit corresponds to a single-site binding model with $K_d = 94.3 \mu\text{M}$ and stoichiometry 0.98.

References:

Jones, S. & J. M. Thornton, (1996) Principles of protein-protein interactions. *Proc Natl*

Acad Sci U S A **93**: 13-20.

Krissinel, E. & K. Henrick, (2005) *Detection of Protein Assemblies in Crystals In:*

CompLife 2005, LNBI 3695, pp. 163--174., p. 163-174. Springer-Verlag, Berlin

Heidelberg. .